INTERNATIONAL JOURNAL OF AUTOMOTIVE SCIENCE AND TECHNOLOGY

2023, VOL. 7, NO:1, 30-36 www.ijastech.org e-ISSN: 2587-0963

Effect of Al5Ti1B Grain Refiner and Al10Sr Modifier on Mechanical Properties and Corrosion Behavior of A360 Alloy

Engin Kocaman[1*] and Selçuk Şirin[2]

0000-0001-5617-3064, 0000-0002-9129-9217

[1]*Department of Aerospace Engineering, Faculty of Engineering, Zonguldak Bulent Ecevit University, Zonguldak, 67100, Turkey*
[2]*Machine and Metal Technologies Program, Sakarya University of Applied Science, Sakarya, Hendek, 54100, Turkey*

Abstract

In this study, the effect of Al5Ti1B grain refiners and Al10Sr modifiers on the mechanical and corrosion properties of the A360 aluminum alloy was investigated. For this purpose, varying amounts of Al5Ti1B grain refiner and Al10Sr modifier were added to the molten A360 alloy and the molten metal was poured into a permanent mold. Subsequently, microstructural investigations, hardness test, tensile strength and corrosion resistance of the samples were examined. The results showed that, the Al5Ti1B grain refiner promotes finer-grained and coaxial solidification. The Al10Sr modifier, broke down the eutectic particles in the microstructure and caused a more homogeneous distribution in the structure. While the tensile strength and corrosion resistance of the alloy increased both the grain refiner and the modifier added to the A360 alloy, a slight decrease in hardness was observed in the alloys to which only the modifier was added.

Keywords: A360, Grain refinement, Hardness, Tensile, Corrosion

Research Article

https://doi.org/10.30939/ijastech..1237345

Received 17.01.2023
Revised 14.02.2023
Accepted 15.02.2023

* Corresponding author
Engin Kocaman
enginkocaman@beun.edu.tr
Address: Department of Aerospace Engineering, Faculty of Engineering, Zonguldak Bulent Ecevit University, Zonguldak, Turkey
Tel: +903722911970

1. Introduction

Aluminum is an element with a metallic character, which has a low density of 2.7 g/cm^3 in pure form and is abundantly found in nature. So that it is the third most common element among all elements and the most abundant element among metallic elements. In addition to the abundance of aluminum, the Al_2O_3 layer formed on the surface gives aluminum excellent oxidation and resistance to many chemicals. This metal, which is quite ductile in its pure form, can be easily machining and forging, and it can be easily produced by casting method thanks to its low melting temperature. However, the strength of pure aluminum has a very low value of 45-50 MPa [1–4]. This value can be increased with addition of alloying elements to aluminum. The alloying elements added to the aluminum improve the manufacturing properties such as castability and machinability, while hardness, strength, wear and corrosion resistance can be increased. In addition, thanks to the alloying elements, the aluminum alloy becomes heat treatable, so that many properties of the alloy can be improved.

Commercially, aluminum alloys are divided into cast aluminum alloys and wrought aluminum alloys. Both cast and wrought aluminum alloys have heat treatable and non-heat treatable groups. In the use of wrought aluminum alloys, properties such as machinability, hardenability by heat treatment and weldability come to the fore, since the final products generally have thinner sections. In cast aluminum alloys, as the name suggests, the castability properties of the alloy come to the fore. Among these alloys, Al-Si alloys have a special place in terms of their usage rate and ease of production by casting method. The main reason for this is that it has a phase diagram showing the eutectic point with aluminum silicon [5,6]. This reduces casting costs, particularly by lowering the melting temperature of alloys near the eutectic point, and at the same time improves the fluidity properties due to the fact that solidification takes place at lower temperatures. Although hypoeutectic, eutectic and hypereutectic Al-Si alloys are used commercially, as mentioned above, alloys near the eutectic point are preferred. The fact that the castability properties of Al-Si alloys are so good has made these alloys frequently preferred in the automotive industry such as engine blocks, piston cylinders, wheels, composite brake discs, and in areas such as aerospace industry and shipbuilding industry [7–12].

The performance of aluminum alloys can be improved by addition of alloying elements, heat treatment and/or mechanical/thermomechanical methods. In addition to these methods, grain refinement method is widely used, especially in cast aluminum alloys, which ensures the elimination of various casting defects, increases the castability properties of the alloy and improves its mechanical

properties [13–15]. In today's foundries, this process is carried out by adding grain refiner master alloys in the form of rods or tablets into the molten alloy. It is thought that, with the addition of grain refiner to the molten alloy, intermetallic structures that can be dissolved in the molten metal in the grain refiner master alloy, semi-soluble or insoluble form a center for heterogeneous nucleation, thus improving the properties of the alloy by providing a finer grained solidification [16,17]. Grain refinement was carried out by adding titanium into molten aluminum in the 1930s [18]. As a result of this process, while the grains exhibit a equaxial solidification, a more homogeneous structure as microstructural is obtained. This has a positive effect on the mechanical properties of the alloy [19,20]. Also, grain refinement is known to be effective in increasing the fatigue resistance of aluminum alloys by reducing porosity and shrinkage [21,22]. Another master alloy modifier used to increase the machinability performance of cast aluminum alloys, not just the mechanical properties [23,24]. Sr, Na or Sb etc. elements are added in order to distribute the eutectic silicon particles formed during the solidification of eutectic Al-Si alloys more homogeneously in the microstructure [25,26]. At the end of the modification process, the primary silicon particles are refined and dispersed more fine and homogeneously in the microstructure. In this way, the machinability properties of the cast part are improved.

Today, although there are many studies on both grain refinement and modification, these studies still continue intensively. One of the important reasons for this is that the mechanism of grain refinement has not been clarified clearly. This situation causes the master alloys to show a different performance compared to the aluminum alloy to which it is applied. On the other hand, studies on the effects of Al5Ti1B and Al10Sr master alloys on the mechanical and corrosion properties of A360 alloy are limited in the literature. In this study, the effects of different ratios of Al5Ti1B grain refiner and Al10Sr modifier added to the A360 alloy on the microstructural, mechanical and corrosive properties of the A360 alloy were investigated, aiming to contribute to the filling of these gaps identified in the literature.

2. Experimental Studies

In this study, primary production aluminum alloy in the form of ingots received from Eti Aluminum Company and given in Table 1 as a result of spectral analysis was used. The alloy in the form of ingots was cut into pieces of 3 kilograms and placed in SiC crucibles and melted at 760 ºC with an electric resistance furnace. According to the design given in Table 2, Al5Ti1B grain refiner and/or Al10Sr modifier were added into the melted alloys and mixed with the help of a graphite rod. After the master alloy was added, the molten metal was kept in the furnace for 10 minutes. At the end of this period, degassing was done for 5 minutes by using nitrogen gas in the furnace with the help of a graphic lance, and then casting was carried out by keeping it waiting for 5 minutes. The casting process was carried out using a permanent mold whose schematic view is given in Figure 1. All casting processes were carried out at mold temperature of 250 ºC and casting temperature of 720 ºC.

Table 1. Spectral analysis of A360 aluminum alloy

Zn	Mg	Cu	Fe	Si	Ni	Ti	Al
0.1	0.33	0.1	0.5	9-10	0.1	0.15	Bal.

Tensile test specimens were prepared on Lokesh-Tl 250 CNC lathe in accordance with ASTM B-108 standards (Figure 1-d). Tensile tests were carried out at room temperature at a speed of 0.5 mm/min using an Alşa Company 10 tons capacity tensile device. Microstructure and corrosion tests were applied to the samples cut by using a water-cooled cutting device from a distance of 10 mm from the base of the cast parts. Microstructure and corrosion samples were prepared by sanding and polishing according to standard metallographic procedures. The samples to be examine microstructurally were etched with Keller's solution. Microstructural examinations of etched samples were carried out using Leica M 1750 optical microscope and Jeol JSM-6060LV scanning electron microscope (SEM).

Table 2. Amount of added master alloys

Master Alloys	Cast 1	Cast 2	Cast 3	Cast 4	Cast 5	Cast 6
Al5Ti1B (ppm)	-	100	200	-	-	200
Al10Sr (ppm)	-	-	-	100	200	200

Hardness measurements were measured in Brinell hardness mode with Bulut Machine DIGIROCK-RB model hardness device by applying a 2.5 mm diameter ball and 62.5 kg load. The average hardness result was determined by taking 10 measurements at 5 mm intervals across the entire surface. Electrochemical corrosion tests were performed with Gamry Interface 1010-E Potentiostat at 25 ºC, in 0.5 M NaCl solution, with a scanning range of -0.5 to +1.5 V and a scanning rate of 1 mV/s. Saturated calomel electrode was used as reference electrode and graphite as counter electrode.

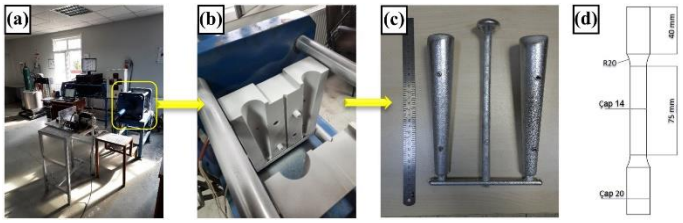

Fig. 1. a) Experimental setup b) Casting press c) Cast Sample d) Tensile test sample

3. Results

3.1 Microstructural Investigation

Optical microscope images of cast samples at different magnifications are given in Figure 2. In the optical microscope image of the Cast 1, which is the reference sample, it is seen that the dendrite sizes are quite large. At high magnifications, it is seen that there are blocky black particles formed in the region between dendrites and solidified in rod-like form. In addition, there are complex shaped structures in light gray color. In the SEM image, EDS and MAP analysis of this sample given in Figure 4, both the blocky

phases and the rod-shaped structures contain high amounts of silicon.

It can be said that the rod-shaped silicons seen in the microstructure are eutectic silicon particles that solidify eutectically. On the other hand, blocky phases can be explained as eutectic silicon particles that become coarse depending on the solidification time or as primary silicon particles formed during solidification. Normally, primary silicon particles are not expected to form in hypoeutectic aluminum-silicon alloys, but it has been reported that primary silicon particles can form in hypoeutectic Al-Si alloys depending on solidification conditions [27]. On the other hand, the light gray colored phases exhibit a morphology similar to the phases containing Al, Si, Fe, and Mg, known as Chinese script in the literature [28]. It is seen that complex shaped phases, similar to these phases but with larger structures, take place in the microstructure. In the MAP analysis given in Figure 4, it is understood that high amounts of Fe and Mn signals were obtained from these phases. In the EDS analysis no. 1 performed right on this phase, it is seen that a high level of aluminum signal and some Fe and Mn signals are obtained. It is reported in the literature that these phases are intermetallic structures with $(FeMn)_3Si_2Al_{15}$ composition [29].

In the optical microscope image of the Cast 2 coded sample in Figure 2, the dendrite lengths are shortened and the distance between the dendrite arms is reduced. In addition, it was determined that α-Al dendrites became equaxial with the added grain refiner. In the grain refinement processes applied to aluminum alloys, the general opinion is that the added Al5Ti1B grain refiner creates soluble, semi-soluble or insoluble intermetallic phases such as $TiAl_3$, AlB_2 and TiB_2 in the melt, and these phases play a role as a heterogeneous nucleation center during solidification [30,31].

In this way, as can be seen from the optical microscope images, the solidification starts at many points in the molten metal and promotes the equaxial solidification of the alloy, thanks to the grain refiner added to the alloy that solidifies as long dendrites. In the 200X magnification image of the same sample, it is understood that there is no visible change in the size of the coarse eutectic silicon particles, but there is a decrease in the number of these particles. In the study performed by Basak et al. [32], 0-6% by weight Al5Ti1B grain refiner was added to the Al-Si alloy containing 12.6% (wt.) Si.

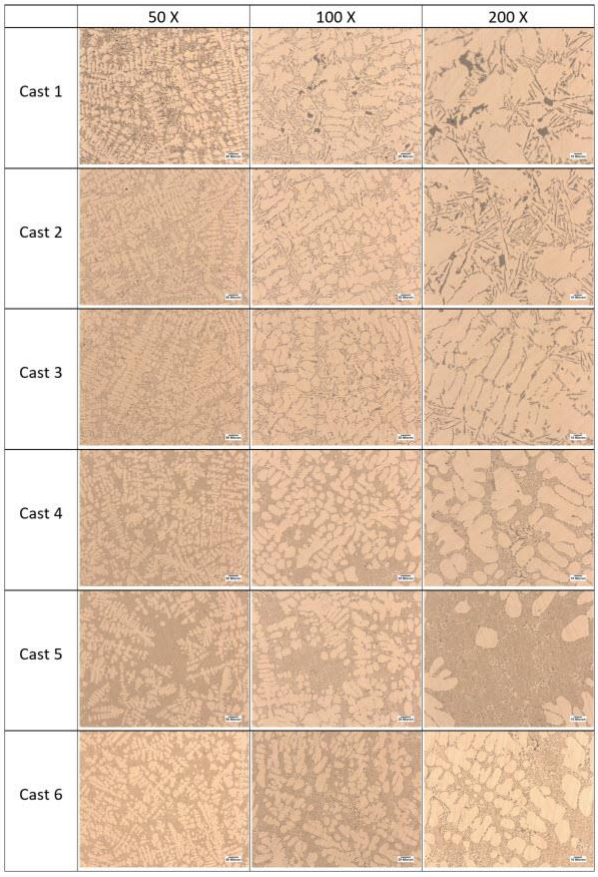

Fig. 2. Optical microscope images of cast samples

It has been reported that as a result of the addition of grain refiner, the coarse silicon particles are surrounded by nano-sized $AlTi_3$, and it inhibits the growth of silicon particles. It is seen that the addition of grain refiner is effective in refining coarse eutectic silicon particles in the samples produced within the scope of experimental studies. However, unlike the study by Başak et al., the use of a much lower rate of grain refiner in the samples produced within the scope of experimental studies caused less growth-restricting effect on coarse eutectic silicon particles. It is understood that there is no visible change in the optical microscope images of the Cast 3 coded sample, which is obtained as a result of doubling the amount of 100 ppm Al5Ti1B grain refiner added to the Cast 2 sample, that is, to 200 ppm, but the size of the coarse eutectic silicon particles has decreased considerably.

In Cast 4 and Cast 5 samples, 100 ppm and 200 ppm Al10Sr modifier were added instead of grain refiner, respectively. In the optical microscope image of these samples, there is no change in the dendrite sizes of the microstructures compared to the reference sample, but the eutectic silicon particles are finer. The eutectic silicon particles exhibited a finer solidification with the increasing Al10Sr modifier in the microstructure of the cast sample 5. In the optical microscope image of casting number 6, obtained by adding 200 ppm Al5Ti1B and 200 ppm Al10Sr into the A360 alloy, it is seen that there is a decrease in dendrites lengths similar to the castings with only grain refiner added.

It is also understood that the modifier added to this sample breaks up the eutectic silicon particles and distributes them more homogeneously in the structure. However, the sizes of eutectic silicon particles are not as small as Cast 4 and Cast 5. In the literature, the Al-B interaction resulting from the use of a boron-containing grain refiner and a strontium-containing modifier has been explained as reducing the effect of both the grain refiner and the modifier [33].

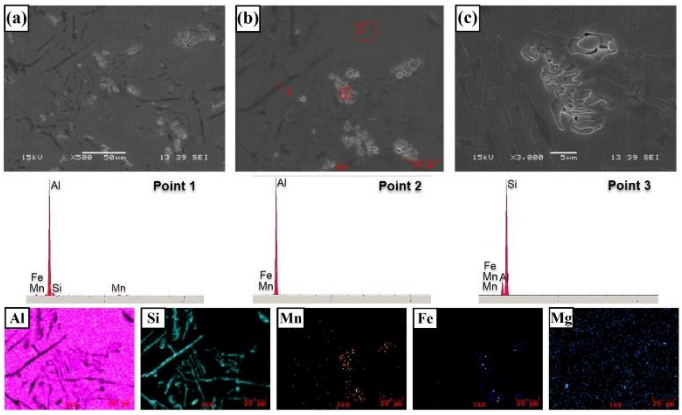

Fig. 3. SEM image, EDS and MAP analysis of sample of Cast 1

For this reason, it is thought that Al5Ti1B grain refiner and Al10Sr modifier in casting number 6 may cause such an effect. On the other hand, this situation is also seen in the SEM images of the samples Cast 3, Cast 5 and Cast 6 given in Figure 5. While the Al5Ti1B grain refiner added to the alloy reduces the arm distance between dendrites and dendrites, it does not cause a significant effect on the eutectic silicon particles. However, it is understood that with the modifier added to the alloy, the eutectic silicon particles are fragmented and dispersed in the structure. It is also seen that there is a decrease in dendrite lengths and a refining in eutectic silicon particles in the microstructure of the alloy, where both the grain refiner and the modifier are used.

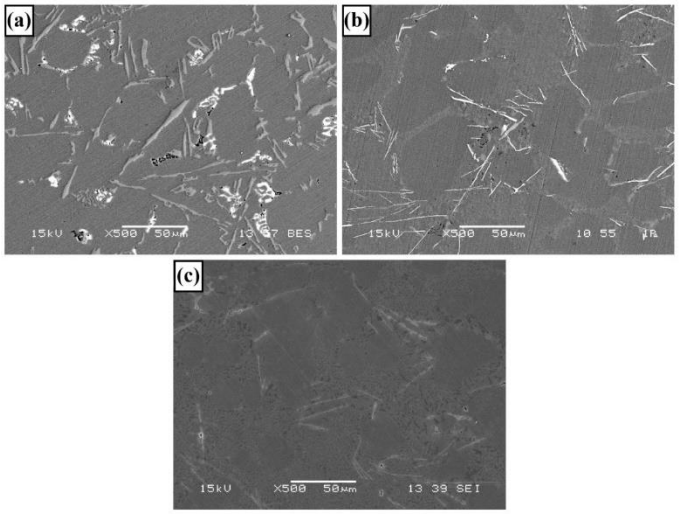

Fig. 4. SEM images of cast samples a) 200ppm Al5Ti1B b) 200ppm Al10Sr c) 200 ppm Al5Ti1B + 200 ppm Al10Sr

3.1 Mechanical Test Results

In Figure 5-a, the hardness values measured using the Brinell hardness method from the cast samples are given. The hardness of the first casting, which is the reference sample, was measured as 60.1 HB. This value is compatible with similar studies carried out in the literature [34]. It has been determined that there is a ~14% increase in the hardness of the alloy with Al5Ti1B grain refiner added to the alloy at a rate of 100 ppm by weight. By increasing the amount of grain refiner to 200 ppm by weight, the hardness value increased by ~10% compared to the initial situation. However, the hardness value did not increase with the increase in the amount of grain refiner. It is seen that the hardness values of Cast 4 and Cast 5 samples decreased slightly compared to the initial situation and did not change with increasing Al10Sr modifier amount. As a result of 200 ppm Al5Ti1B and 200 ppm Al10Sr added into the alloy in Casting 6 sample, the hardness value increased compared to the initial situation, but remained lower than Casting 3 and Casting 4 samples, where only grain refiner was added. With the addition of grain refiner, it is expected that the hardness will increase as a result of the increase in the number of grains that can prevent the dislocation movement in the microstructure. On the other hand, with the addition of modifier, eutectic silicon particles exhibit a finer and homogeneous distribution. In the absence of grain refiner, a more refined and homogeneous microstructure is expected to increase ductility along with strength. For this reason, a partial decrease in the hardness value occurred with the addition of the modifier. In a similar study, Fan et al. [35] reported that the hardness of the alloy decreased with the increase in the amount of Al10Sr modifier added at different rates to the aluminum alloy containing 10-13 wt% Si. It has been reported that the SrB6 phase formed when the boron in the Al5Ti1B grain refiner and the Sr in the modifier are Sr/B=1.35 reduce both the effect of the grain refiner and the modifier by binding the strontium and boron [33]. For this reason, the hardness of the casting number 6 was lower than the hardness values of the Cast 2 and Cast 3 samples, in which only Al5Ti1B grain refiner was added.

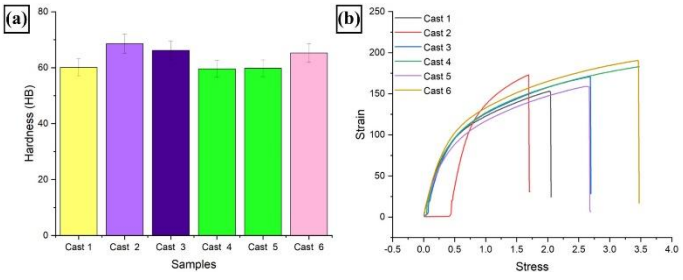

Fig. 5. a) Hardness and b) Tensile test results

The tensile test results applied to the cast specimens are given in Figure 5-b. The tensile strength of the reference sample was measured as ~153 MPa. With the addition of 100 ppm Al5Ti1B into the A360 alloy, the tensile strength increased by ~13.1% compared to the reference sample and was measured as 173 MPa. However, by increasing the amount of grain refiner to the level of 200 ppm, it was determined that the tensile strength value increased compared

to the reference sample and decreased compared to the sample with 100 ppm grain refiner added. In the Cast 4 and Cast 5 samples, the Al10Sr modifier added to the alloy increased the tensile strength and % elongation values compared to the initial value of the A360 alloy. However, a decrease in the tensile strength value of the cast part occurred as a result of increasing the addition rate from 100 ppm to 200 ppm, similar to the grain refiner master alloy. In the literature, a study was conducted by Fan et al. [35] to examine the effect of the amount of modifier on ZL102 aluminum alloy. In the study, it was reported that the silicon refining formed in the microstructure as a result of increasing the amount of modifier will increase the strength and ductility. As a result of decreasing in grain size caused by grain refiner added into A360 alloy, dislocation movement is restricted and causes an increase in hardness and strength as stated in Orawan and Hall-Patch theories [36–38]. On the other hand, it is seen that there is no increase in hardness and strength with increasing amount of grain refiner. This can be explained by the changes in the microstructure of the increasing master alloy addition.

In a similar study, Rodriguez et al. [39] investigated the effect of Al5Ti1B grain refiner added to the Al-Si-Fe alloy between 0-0.03% by weight on the mechanical properties of the alloy. In the study, it was shown that increasing amount of grain refiner did not cause a significant change in the tensile strength of Al-12Si-0.44Fe alloy, and this was explained by the absence of a significant change in microstructure with increasing grain refiner. In a similar study, Samuel et al. [40] found a decrease in the strength value of the A356.2 alloy with increasing master alloy. Samuel et al. explained this situation as intermetallic phases such as titanium-based $TiAl_3$ and TiB_2 can agglomerate in certain regions in the microstructure and have an adverse effect on the mechanical properties. The highest tensile strength and ductility values obtained in experimental studies were obtained in casting number 6. The change in the microstructure of Al5Ti1B master alloy and Al10Sr at a rate of 200 ppm added into the molten alloy played a role in increasing the tensile strength and ductility.

3.3. Corrosion Test Results

Tafel curves obtained as a result of the potentiodynamic polarization test are given in Figure 6. It is understood that the Tafel curves are very close to each other and the corrosion potential values vary between -573.5 and -605.5 mV, as can be seen from the Tafel parameters given in Table 3. On the other hand, it is understood that there is no linear change in corrosion potentials with Al5Ti1B grain refiner or Al10Sr modifier added to the A360 alloy. It is seen that the most noble alloy among the samples produced according to their corrosion potential is the Cast 6. Uludağ et al. [41], who carried out a similar study in the literature, reported that the grain refiner and modifier added to the Al-7Si-0.3Mg alloy did not cause a significant change in the corrosion potential of the samples. However Yaman et all [42] reported that grain refiner has positive effect on corrosion resistance of Al 7075 alloy.

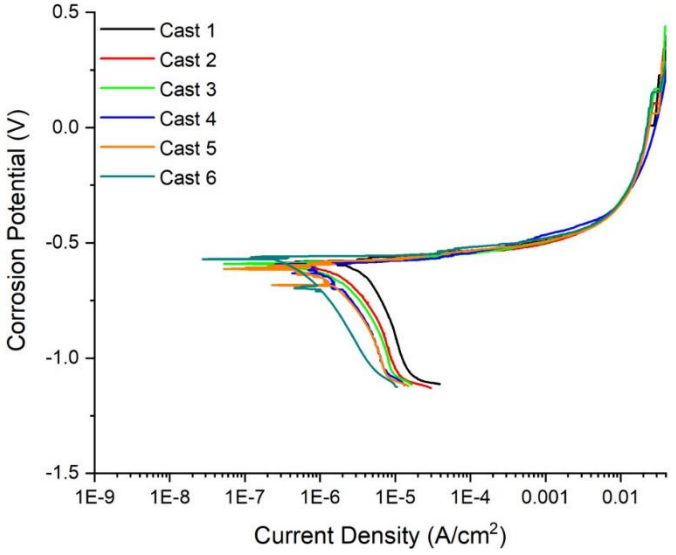

Fig. 6. Tafel curve of cast samples

When the corrosion tests in the Tafel parameters given in Table 3 and especially the current density values, which is a critical parameter in terms of kinetics, are examined, it is understood that the highest current density was measured in casting number 1, and the lowest current density was measured in Cast 6. Similarly, in the corrosion rate values, it is understood that the highest corrosion rate was measured in the reference sample and the lowest corrosion rate was measured in the Cast 6. Although there is no clear view on the corrosion resistance of the alloy in grain refinement studies, some researchers stated that the corrosion resistance increases with decreasing grain size, while others stated that larger grain size is required for higher corrosion resistance [43–45]. In this study, the corrosion resistance of the alloy increased slightly with the addition of grain refiner. Also, addition of modifier to the A360 alloy increases the corrosion resistance of the alloy. In the literature, the studies have shown that the addition of a modifier will increase the corrosion resistance as a more refined microstructure is obtained [46]. It is seen that the findings obtained within the scope of experimental studies are compatible with the literature.

Table 3. Material properties of SCP10.

Sample	Ecor (mV)	Icor (μA/cm^2)	βa (V/dec)	βc (V/dec)	Cr (mpy)
Cast 1	-579.3	2.503	28.6	337.8	1.357
Cast 2	-588.9	1.478	23.9	377.7	0.801
Cast 3	-592.8	1.225	22.9	363.2	0.669
Cast 4	-591.8	1.039	12.8	391	0.563
Cast 5	-605.5	0.95	35.3	363.3	0.515
Cast 6	-573.5	0.45	15.2	409.3	0.244

4. Conclusions

In this study, the effects of Al5Ti1B grain refiner and Al10Sr modifier added to the A360 alloy at different rates on the microstructure, hardness value, tensile strength and corrosion resistance of the alloy were investigated and the findings are as follows;

With the Al5Ti1B grain refiner added to the A360 alloy, it was observed that the dendrite lengths were shortened compared to the reference sample, and the transition from dendritic solidification to a equaxial solidification was observed. With the Al10Sr modifier added into the alloy, the eutectic silicon particles were fragmented and showed a refined distribution in the structure. Grain size reduction and refining of eutectic silicon particles occurred as a result of the addition of both grain refiner and modifier to the molten alloy.

Al5Ti1B grain refiner added to the A360 alloy increased the hardness value of the alloy by approximately 10-14% compared to the initial situation. Al10Sr modifier reduced the hardness of the alloy slightly compared to the initial state. On the other hand, it was observed that the hardness test results for both the grain refiner and the modifier changed independently of the addition amount.

According to the tensile test result, the tensile strength and ductility of the alloy to which Al5Ti1B grain refiner was added increased compared to the initial situation. While the tensile strength and elongation values increased with the addition of the modifier, it was observed that the modifier was more effective on the elongation of the alloy. In the study, the highest tensile strength and elongation values were obtained in Casting 6, where both master alloys were used at a rate of 200 ppm.

According to the potentiodynamic polarization test results, both the grain refiner and the modifier shifted the corrosion potential values of the samples to the nobler side and decreased the current density values. In the study, the highest corrosion potential, the lowest current density and the highest corrosion resistance value were obtained in the Cast 6, in which both grain refiner and modifier were added.

Acknowledgment

This study was supported by Zonguldak Bulent Ecevit University Scientific Research Projects Coordinatorship project numbered BAP 2021-73338635-01.

Conflict of Interest Statement

The authors declare that there is no conflict of interest in the study.

CRediT Author Statement

Engin Kocaman: Conceptualization, Data curation, Writing-original draft, Project administration,
Selçuk Şirin: Conceptualization, Writing-original draft, Validation,

References

[1] Mondolfo LF. Aluminum Alloys: Structure and Properties. Butterworth-Heinemann;1976. https://doi.org/https://doi.org/10.1016/B978-0-408-70932-3.50010-3.

[2] Brandes EA, Brook GBBT-SLMH, editors. 2 - General physical properties of light metal alloys and pure light metals, Oxford: Butterworth-Heinemann; 1998,5–13. https://doi.org/https://doi.org/10.1016/B978-075063625-4/50002-8.

[3] Krishnaiah A, Chakkingal U, Kim HS. Mechanical properties of commercially pure aluminium subjected to repetitive bending and straightening process. Trans Indian Inst Met 2008;61:165–7. https://doi.org/10.1007/s12666-008-0032-3.

[4] Kammer C. Aluminum and Aluminum Alloys BT - Springer Handbook of Materials Data. In: Warlimont H, Martienssen W, editors., Cham: Springer International Publishing; 2018, p. 161–97. https://doi.org/10.1007/978-3-319-69743-7_6.

[5] Warmuzek M. Aluminum-silicon casting alloys. Ohio: ASM International; 2004.

[6] Miao Q, Wu D, Chai D, Zhan Y, Bi G, Niu F, et al. Comparative study of microstructure evaluation and mechanical properties of 4043 aluminum alloy fabricated by wire-based additive manufacturing. Mater Des 2020;186:108205. https://doi.org/https://doi.org/10.1016/j.matdes.2019.108205.

[7] Starke EA. 2 - Heat-Treatable Aluminum Alloys. In: Vasudevan AK, Doherty RDBT-T on MS& T, editors. Alum. Alloy. Res. Appl., vol. 31, Elsevier; 1989, p. 35–63. https://doi.org/https://doi.org/10.1016/B978-0-12-341831-9.50007-3.

[8] Stojanovic B, Bukvic M, Epler I. Application of aluminum and aluminum alloys in engineering. Appl Eng Lett 2018;3:52–62. https://doi.org/10.18485/aeletters.2018.3.2.2.

[9] Hilpert E, Hartung J, von Lukowicz H, Herffurth T, Heidler N. Design, additive manufacturing, processing, and characterization of metal mirror made of aluminum silicon alloy for space applications. Opt Eng 2019;58:1. https://doi.org/10.1117/1.oe.58.9.092613.

[10] Graf A. Chapter 3 - Aluminum alloys for lightweight automotive structures. In: Mallick Design and Manufacturing for Lightweight Vehicles (Second Edition) PKBT-M, editor. Woodhead Publ. Mater., Woodhead Publishing; 2021, p. 97–123. https://doi.org/https://doi.org/10.1016/B978-0-12-818712-8.00003-3.

[11] Uslu E, Çatar R, Çolak M. Si VE Cu Elementlerini İçeren Aluminyum Döküm Alaşımlarının Korozyon Özelliklerinin Belirlenmesi ve Karşılaştırılması. Journal 2017;12:133–40.

[12] Miladinovic S, Gajević S, Ivanović L, Skulić A, Stojanović B. A review of hypereutectic aluminum piston materials. IOP Conf Ser Mater Sci Eng 2022;1271:12012. https://doi.org/10.1088/1757-899X/1271/1/012012.

[13] Dahle AK, Arnberg L. Development of strength in solidifying aluminium alloys 1997;45:547–59. https://doi.org/https://doi.org/10.1016/S1359-6454(96)00203-0.

[14] Çolak M, Yetgin SH. Investigation of the Effects of Casting Method on Cooling Plate on Tribological Properties of A357 Aluminum Alloy with Taguchi Method 2018;7:99–103.

[15] Kayikci R, Colak M, Sirin S, Kocaman E, Akar N. Determination of the critical fraction of solid during the solidification of a PM-cast

aluminium alloy. Mater Tehnol 2015;49:797–800. https://doi.org/10.17222/mit.2014.266.

[16] Çolak M, Kayıkcı R. Alüminyum Dökümlerinde Tane İnceltme. SAÜ Fen Bilim Enstitüsü Derg 2009;13:11–7.

[17] Savaş Ö, Kayikci R. A Taguchi optimisation for production of Al–B master alloys using boron oxide. J Alloys Compd 2013;580:232–8. https://doi.org/https://doi.org/10.1016/j.jallcom.2013.05.112.

[18] Eser UA. Alümiyum ve Silisyum Alaşımlarında Bor İle Tane İnceltme. Yıldız Teknik Üniversitesi, 2019.

[19] Teke, Çolak M, Taş M, İpek M. Modeling of the impact of initial mold temperature, Al5Ti1B and Al10Sr additions on the critical fraction of solid in die casting of aluminum alloys using fuzzy expert system. Acta Phys Pol A 2019;135:1105–7. https://doi.org/10.12693/APhysPolA.135.1105.

[20] Kocaman E, Şirin S, Dispinar D. Artificial Neural Network Modeling of Grain Refinement Performance in AlSi10Mg Alloy. Int J Met 2020. https://doi.org/10.1007/s40962-020-00472-9.

[21] Samuel AM, Mohamed SS, Doty HW, Valtierra S, Samuel FH. Effect of melt temperature on the effectiveness of the grain refining in Al-Si castings. Adv Mater Sci Eng 2018;2018. https://doi.org/10.1155/2018/7626219.

[22] Çolak M, Dışpınar D. Taguchi Approach for Optimization of Parameters that Effect Grain Size of Cast A357 Alloy. Arch Foundry Eng 2017;17:35–42. https://doi.org/10.1515/afe-2017-0127.

[23] Çolak M. Modification of eutectic Al–Si alloys by Sr and CuSn5. Mater Res Express 2019;6:1065a2. https://doi.org/10.1088/2053-1591/ab3c0f.

[24] Muhammet U, Yazman Ş, Bakırcıoğlu B, Dışpınar D. Al-Si Alaşımlarında Si Morfolojisinin İşlenebilirliğe Etkisi. Journal 2016;21:381–5.

[25] Arslan İ, Gavgalı E, Çolak M. Kum Kalıba Dökülen Farklı Alüminyum Alaşımlarının Dökümünde Al5Ti1B ve AL10SR İlavesinin Mikroyapı Özelliklere Etkisinin İncelenmesi. Acad Platf J Eng Sci 2019;7:237–44. https://doi.org/10.21541/apjes.424920.

[26] FundaKahraman M. Microstructure and Eutectic Morphology of Al-12.5°/O Si Alloy Refined with Antimony. Journal 2007;11:10–4.

[27] Wang SR, Ma R, Wang YZ, Wang Y, Yang LY. Growth mechanism of primary silicon in cast hypoeutectic Al-Si alloys. Trans Nonferrous Met Soc China (English Ed 2012;22:1264–9. https://doi.org/10.1016/S1003-6326(11)61314-9.

[28] Liu YL, Kang SB, Kim HW. Complex microstructures in an as-cast Al-Mg-Si alloy. Mater Lett 1999;41:267–72. https://doi.org/10.1016/S0167-577X(99)00141-X.

[29] Bassani P, Previtali B, Tuissi A, Vedani M, Vimercati G, Arnaboldi S. Solidification behaviour and microstructure of A360-SIC P cast composites. Metall Sci Technol 2005:3–10.

[30] Easton MA, Stjohn DH. Grain refinement of aluminum alloys : Part I . The nucleant and solute paradigms — A review of the literature. Metall Mater Trans A 1999;30:1613–23. https://doi.org/10.1007/s11661-999-0098-5.

[31] Sigworth GK, Kuhn TA. Grain refinement of aluminum casting alloys 2007.

[32] Basak S, Biswas P, Patra S, Roy H, Mondal MK. Effect of TiB2 and Al3Ti on the microstructure, mechanical properties and fracture behaviour of near eutectic Al-12.6Si alloy. Int J Miner Metall Mater 2021;28:1174–85. https://doi.org/10.1007/s12613-020-2070-8.

[33] Samuel A, Doty H., Valtierra S, Samuel F. Effect of grain refining and Sr-modification interactions on the impact toughness of Al–Si–Mg cast alloys. Mater Des 2014;56:264–73. https://doi.org/https://doi.org/10.1016/j.matdes.2013.10.029.

[34] Kosgey BK, Maranga SM, Kihiu JM, Ando Y. Investigation on Hardness of Gravity Die Cast Secondary Al-10Si Piston Alloy with Trace Addition of Sr , Fe and Mn 2014;1:51–6.

[35] Fan B, Mo J, Zhang J, Shen H, Liu R. Effect of Sr Modifier on Microstructure and Mechanical Properties of ZL102 Casting Suspension Clamp. IOP Conf Ser Earth Environ Sci 2020;525:1–6. https://doi.org/10.1088/1755-1315/525/1/012159.

[36] Hornbogen E. Hundred years of precipitation hardening. J Light Met 2001;1:127–32. https://doi.org/https://doi.org/10.1016/S1471-5317(01)00006-2.

[37] Xie X, Shen J, Cheng L, Li Y, Pu Y. Effects of nano-particles strengthening activating flux on the microstructures and mechanical properties of TIG welded AZ31 magnesium alloy joints. Mater Des 2015;81:31–8. https://doi.org/https://doi.org/10.1016/j.matdes.2015.05.024.

[38] Deng J, Shen J, Li H, Chen H, Xie F. Investigation on microstructure, mechanical properties and corrosion behavior of Sc-contained Al-7075 alloys after solution-Aging treatment. Mater Res Express 2020;7. https://doi.org/10.1088/2053-1591/abb4fa.

[39] Rodríguez SH, Goytia Reyes RE, Dwivedi DK, González OA, Hernández VHB. The effect of Al-5Ti-1B on microstructure and mechanical properties of Al-12Si-xFe alloy. Mater Manuf Process 2012;27:599–604. https://doi.org/10.1080/10426914.2011.560230.

[40] Samuel E, Golbahar B, Samuel AM, Doty HW, Valtierra S, Samuel FH. Effect of grain refiner on the tensile and impact properties of Al–Si–Mg cast alloys. Mater Des 2014;56:468–79. https://doi.org/https://doi.org/10.1016/j.matdes.2013.11.058.

[41] Uludağ M, Kocabaş M, Dışpınar D, Çetin R, Cansever N. Effect of Sr and Ti addition on the corrosion behaviour of Al-7Si-0.3Mg alloy. Arch Foundry Eng 2017;17:125–30. https://doi.org/10.1515/afe-2017-0063.

[42] Yaman MB, Kocaman E, Avar B. Al7075 Alaşımına İlave Edilen Al-5Ti-1B Tane İncelticinin Yaşlanma, Mikroyapı, Sertlik ve Korozif Özellikleri Üzerindeki Etkisi. Journal 2022;10:870–83. https://doi.org/https://doi.org/10.29109/gujsc.1165103.

[43] Ralston KD, Birbilis N, Davies CHJ. Revealing the relationship between grain size and corrosion rate of metals. Scr Mater 2010;63:1201–4. https://doi.org/https://doi.org/10.1016/j.scriptamat.2010.08.035.

[44] Son I, Nakano H, Oue S, Kobayashi S, Fukushima H, Horita Z. Effect of Equal-Channel Angular Pressing on Pitting Corrosion of Pure Aluminum. Int J Corros 2012;2012:450854. https://doi.org/10.1155/2012/450854.

[45] El-Aziz KA, Ahmed EM, Alghtani AH, Felemban BF, Ali HT, Megahed M, et al. Development of Al–Mg–Si alloy performance by addition of grain refiner Al–5Ti–1B alloy. Sci Prog 2021;104. https://doi.org/10.1177/00368504211029469.

[46] Öztürk İ, Ağaoğlu GH, Erzi E, Dispinar D, Orhan G. Effects of strontium addition on the microstructure and corrosion behavior of A356 aluminum alloy. J Alloys Compd 2018;763:384–91. https://doi.org/https://doi.org/10.1016/j.jallcom.2018.05.341.